Differentiable Rendering Framework for Retroreflective Model Construction in Mid-Air Image Simulation

Ryo Sugawara
The University of Electro-Communications
Chofu, Japan
sugawara.ryo@media.lab.uec.ac.jp

Naoya Koizumi
The University of Electro-Communications
Chofu, Japan
koizumi.naoya@uec.ac.jp

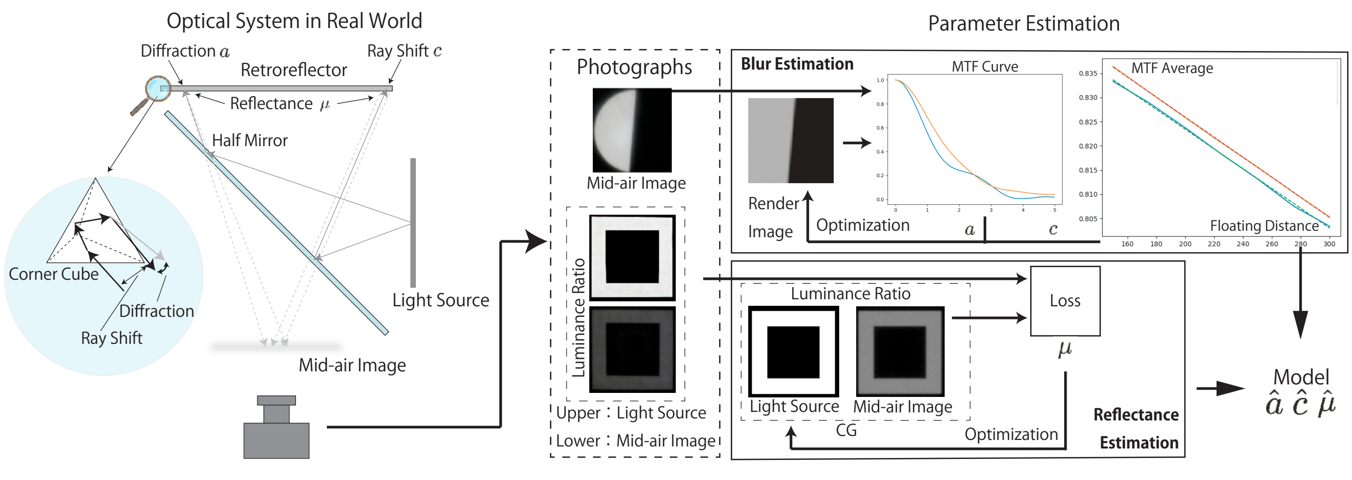

Figure 1: Overview of the proposed method.

Abstract

This paper presents a differentiable rendering framework for constructing accurate retroreflective models used in mid-air image simulation. Simulating mid-air images requires precise reproduction of luminance and blur characteristics that vary with viewing angle and floating distance. Our method estimates optical parameters directly from photographs of mid-air images, enabling accurate reproduction of these effects without physical prototyping. Experimental results show that our model reproduces mid-air images similar to real photographs, achieving higher similarity to real photographs than conventional models according to LPIPS metric.

ACM Reference Format:

Ryo Sugawara and Naoya Koizumi. 2025. Differentiable Rendering Framework for Retroreflective Model Construction in Mid-Air Image Simulation. In *SIGGRAPH Asia 2025 Posters (SA Posters '25), December 15–18, 2025, Hong Kong, Hong Kong*. ACM, New York, NY, USA, 3 pages. https://doi.org/10.1145/3757374.3771778

1 Introduction

Mid-air imaging displays visible images directly in space without screens or head-mounted displays, enabling new applications in public installations and interactive displays. Among various techniques, Aerial Imaging by Retro-Reflection (AIRR) [Yamamoto et al. 2014] achieves wide viewing angles and scalability using corner-cube retroreflectors and half mirrors. However, the blur and luminance attenuation of AIRR images cannot be fully predicted without assembling the optical system, highlighting the need for a simulation-based approach to estimate these effects in advance.

This study proposes a differentiable rendering framework to estimate retroreflector parameters from photographs of mid-air images. This approach enables designers to predict the appearance of large-scale mid-air images, such as those used on stage installations, to pre-evaluate visibility for applications like signage, and to design complex optical configurations for biological experiments before physical implementation.

2 Related work

Simulating mid-air images in computer graphics (CG) enables optical system design without physical prototyping [Kiuchi and Koizumi 2021], [Hoshi et al. 2022]. Previous AIRR studies modeled retroreflection via geometric optics, Guo et al. [Guo et al. 2018] proposed a BRDF for corner-cube arrays, and Saito et al. [Saito et al. 2024] introduced a microfacet model; however, both lacked precise blur reproduction. Differentiable rendering [Jakob et al. 2022; Vicini et al. 2021] offers a promising way to estimate such parameters efficiently, which motivates our approach. We modeled the AIRR retroreflector following Kakinuma et al. [Kakinuma et al. 2021], who identified diffraction and ray shifts in the corner-cube array as the main causes of luminance loss and blur.

SA Posters '25, Hong Kong, Hong Kong

ACM ISBN 979-8-4007-2134-2/25/12
https://doi.org/10.1145/3757374.3771778

3 Method

We developed a retroreflective model that integrates diffraction-based blur and ray-shift simulation. The squared sinc function describes the intensity distribution of diffracted light, the reflectance model is as follows

$$f(\theta_i, \theta_o) = \mu \frac{\sin^2(aR\tan(\theta_o - \theta_i))}{(aR\tan(\theta_o - \theta_i))^2}, \quad (1)$$

where μ denotes reflectance, a the diffraction spread, and R the floating distance. Ray-shift distributions were precomputed using Mitsuba 3 [Jakob et al. 2022] and stored in lookup tables.

Ray shifts were simulated using Mitsuba 3 [Jakob et al. 2022] with a physically accurate corner-cube geometry. Rays incident at varying angles were traced through the three reflective faces, and their exit-point deviations were recorded to form a probabilistic shift distribution. These distributions, parameterized by the incident angle, were stored in a lookup tables and used during rendering to perturb outgoing rays. The corner-cube edge length was normalized to unity, allowing the shift to be scaled later by the corner size c.

Parameter estimation uses differentiable rendering to minimize differences between real and simulated mid-air images. First, parameters a (Eq. (1)) and c (ray shift) are jointly estimated following the flow in Fig. 1. After initialization, a CG mid-air image is rendered with an edge image as the light source, and its MTF is calculated. Once geometric parameters are fixed, reflectance μ is optimized to match the luminance ratio between the source and mid-air image.

Loss functions are based on mean-squared error for MTF and luminance ratio differences. Optimization typically converges in fewer than 200 iterations. For efficiency, simulations were executed at a resolution of 512×512 pixels with 256 samples per pixel. The differentiable rendering loop was parallelized across incident angles (0°–45° in 5° increments).

The physical setup for image capture used a white LED light source with an integrating sphere (Labsphere 3P-GPS-040-SF), a half mirror and two retroreflectors (RF-Ay, RF-AN). Images were captured using a camera (Sony α7R V) equipped with a 24–105 mm F4 lens, at ISO 100, f/4.0, and 1/13 s exposure. The same geometry and illumination parameters were reproduced in CG for validation, ensuring consistent brightness and blur measurement between real and simulated conditions.

4 Evaluation

We compared simulated and real mid-air images under various distances and incident angles.

The proposed model preserved fine edge contrast and reduced over-blurring around bright regions. These results confirm that the differentiable optimization successfully adjusted diffraction and ray-shift parameters to match real optical behavior, demonstrating the practicality of the approach for AIRR design.

LPIPS [Zhang et al. 2018] was used as an image similarity metric. As listed in Table 1, the LPIPS values obtained with our model were lower than those of Saito et al.'s model. A lower LPIPS value indicates a higher similarity to the real mid-air image, suggesting greater simulation accuracy. LPIPS improved from 0.39 to 0.31 on average for RF-Ay and from 0.37 to 0.29 for RF-AN. This improvement corresponds to a perceptual similarity increase of approximately 20%.

Table 1: LPIPS comparison between the proposed and conventional models for RF-Ay and RF-AN retroreflectors. Lower values indicate higher similarity to real mid-air images.

Retroreflector	Distance	Method	Image 1	Image 2	Image 3
RF-Ay	150 mm	Proposed	0.319	0.284	0.331
		Saito et al.	0.400	0.353	0.403
	300 mm	Proposed	0.333	0.296	0.349
		Saito et al.	0.398	0.341	0.450
RF-AN	150 mm	Proposed	0.311	0.263	0.300
		Saito et al.	0.379	0.351	0.385
	300 mm	Proposed	0.325	0.277	0.314
		Saito et al.	0.377	0.324	0.395

Figure 2: Example renderings for RF-Ay at floating distances of 150 mm and 300 mm.

Figure 2 shows representative renderings under RF-Ay and RF-AN conditions at floating distances of 150 mm and 300 mm. In Saito et al.'s model, the simulated blur increased excessively with distance, while our model reproduced the real image sharpness transition more accurately.

5 Conclusion

Our method enables accurate, data-driven modeling of retroreflective elements using only photographs. It eliminates the need for specialized measurement setups, broadening access to high-fidelity AIRR simulation for optical designers and content creators. Future work includes extending the model to account for anisotropy and microstructural variations.

Acknowledgments

This work was supported by JST FOREST Program, Grant Number JPMJFR216L.

References

Jie Guo, Yan-wen Guo, and Jin-gui Pan. 2018. A retroreflective BRDF model based on prismatic sheeting and microfacet theory. *Graphical Models* 96 (2018), 38–46. https://doi.org/10.1016/j.gmod.2018.01.002

Ayami Hoshi, Shunji Kiuchi, and Naoya Koizumi. 2022. Simulation of mid-air images using combination of physically based rendering and image processing. *Optical*

Review 29, 2 (March 2022), 106–117. https://doi.org/10.1007/s10043-022-00729-0

Wenzel Jakob, Sébastien Speierer, Nicolas Roussel, and Delio Vicini. 2022. Dr.Jit: A Just-In-Time Compiler for Differentiable Rendering. *Transactions on Graphics (Proceedings of SIGGRAPH)* 41, 4 (July 2022). https://doi.org/10.1145/3528223.3530099

Ryota Kakinuma, Norikazu Kawagishi, Masaki Yasugi, and Hirotsugu Yamamoto. 2021. Influence of incident angle, anisotropy, and floating distance on aerial imaging resolution. *OSA Continuum* 4, 3 (Mar 2021), 865–878. https://doi.org/10.1364/OSAC.416504

Shunji Kiuchi and Naoya Koizumi. 2021. Simulating the appearance of mid-air imaging with micro-mirror array plates. *Computers & Graphics* 96 (2021), 14–23. https://doi.org/10.1016/j.cag.2021.02.007

Asahi Saito, Yonghao Yue, and Naoya Koizumi. 2024. Simulating the Appearance of Aerial Images formed by Aerial Imaging by Retroreflection. *Optical Review* 31, 4 (2024), 395–408. https://doi.org/10.1007/s10043-024-00895-3

Delio Vicini, Sébastien Speierer, and Wenzel Jakob. 2021. Path replay backpropagation: differentiating light paths using constant memory and linear time. *ACM Trans. Graph.* 40, 4, Article 108 (July 2021), 14 pages. https://doi.org/10.1145/3450626.3459804

Hirotsugu Yamamoto, Yuka Tomiyama, and Shiro Suyama. 2014. Floating aerial LED signage based on aerial imaging by retro-reflection (AIRR). *Opt. Express* 22, 22 (Nov 2014), 26919–26924. https://doi.org/10.1364/OE.22.026919

Richard Zhang, Phillip Isola, Alexei A. Efros, Eli Shechtman, and Oliver Wang. 2018. The Unreasonable Effectiveness of Deep Features as a Perceptual Metric. In *2018 IEEE/CVF Conference on Computer Vision and Pattern Recognition*. 586–595. https://doi.org/10.1109/CVPR.2018.00068